Mathematics and Computer Science
2025; 10(5): 83-91
http://www.sciencepublishinggroup.com/j/mcs
doi: 10.11648/j.mcs.20251005.11

Segmentation-Driven Glaucoma Classification from Retinal Fundus Images Using Optic Disk Localization, Linear and Nonlinear Multiple Instance Learning Frameworks

Mahbub Hasan*

Department of Computer Science and Engineering, Southeast University, Dhaka, Bangladesh

Email address:
mahbub.hasan@seu.edu.bd (Mahbub Hasan)
*Corresponding author

To cite this article:
Mahbub Hasan. (2025). Segmentation-Driven Glaucoma Classification from Retinal Fundus Images Using Optic Disk Localization, Linear and Nonlinear Multiple Instance Learning Frameworks. *Mathematics and Computer Science, 10*(5), 83-91.
https://doi.org/10.11648/j.mcs.20251005.11

Received: 24 August 2025; **Accepted:** 4 September 2025; **Published:** 25 September 2025

Abstract: In recent years, glaucoma has been one of the leading causes of vision loss, and its early detection is essential for preventing irreparable damage. This study proposes an efficient classification approach using segmentation on retinal fundus images from the MESSIDOR dataset, focusing on optic disk segmentation to enhance disease-specific feature extraction while minimizing irrelevant background information. The pipeline includes preprocessing steps such as image resizing and green channel extraction, followed by segmentation of both the optic cup and optic disk using traditional image processing techniques, including pixel clustering with superpixel methods, global thresholding, and the Circular Hough Transform (CHT). Performance is evaluated using metrics such as testing correctness (TC), sensitivity, specificity, F1-score, and computational time under 5-fold, 10-fold, and Leave-One-Out (LOO) cross-validation (CV). Results show that preprocessing significantly improves accuracy across all models, with mi-SPSVM under 10-fold CV achieving the best results, obtaining 90.00% sensitivity and a 67.09% F1-score. Meanwhile, mi-KSPSVM achieved the lowest computational time, processing a single image in just 0.09s. These findings demonstrate that incorporating segmentation into the classification task can enhance both diagnostic accuracy and computational efficiency, making the approach suitable for real-time applications and resource-limited environments. Overall, this study presents a promising and scalable solution for automated OD screening, with future work aimed at integrating deep learning-based segmentation to improve precision further.

Keywords: Optic Disk, Optic Cup, Segmentation, Classification, Multiple Instance Learning, Machine Learning, Glaucoma

1. Introduction

Automated retinal image analysis helps to detect earlier severe eye diseases such as glaucoma and diabetic retinopathy (DR), which can cause permanent vision loss. Glaucoma is a lethal disease that harms the optic disc (OD) and optic nerves, often leading to blindness without the patient noticing it early. This damage usually occurs due to high eye pressure. The human eye has a normal pressure level from 10 to 21 millimeters of mercury (mmHg). When the pressure goes above 21 mmHg, it damages the head of the optic nerve inside the optic disc (OD). Ophthalmologists often check features such as the optic disc (OD), optic cup (OC), optic nerve head (ONH), and the cup-to-disc ratio (CDR) to identify diseases such as glaucoma, diabetic retinopathy, and macular edema in the prior stages [5]. Manually checking these characteristics requires highly trained ophthalmologists, which is a limitation and time-consuming. Automated systems can help make the process faster and more accurate. Many techniques use optic disc features like its shape & size of disk, and brightness for detecting glaucoma. The OD is the most luminous circular area in the eye. It is essential in diagnosing not only glaucoma but also conditions like retinal lesions. Automatically finding and segmenting the optic disc is difficult because its appearance can change due to problems such as microaneurysms and luminous spots like hard and soft exudates. Over the years, many methods have been developed for locating the OD, segmenting the OD and OC, and calculating the CDR to detect glaucoma. Figure 1 illustrates the optic disk biomarker from a fundus image.

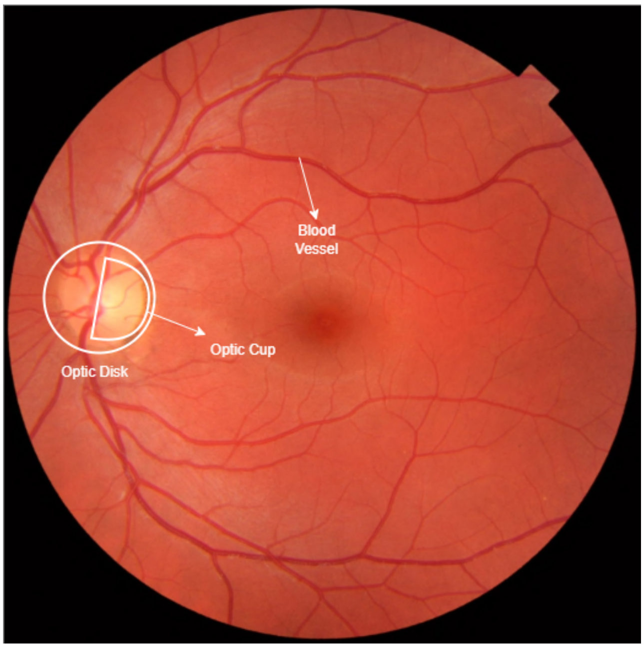

Figure 1. *An important biomarker of fundus image.*

The main objective of this work is to perform optic disc segmentation through image processing techniques and improve classification results through multiple instance learning (MIL) methods using these segmented images. This method is to help ophthalmologists detect glaucoma and retinal disease in its early stages. The challenges and work done are the following:

1. Instead of using a full fundus image, an optic disk segmented image obtains a high sensitivity of 86.69% in an average of three types of cross-validation processes.
2. The whole procedure from optic disk segmentation and mathematical models, explained thoroughly with an algorithm and equations, will help researchers to develop further.
3. The marginal number of images was analyzed using the unsupervised approach and obtained high sensitivity, making the suggested segmentation approach a better fit for the diagnosis of glaucoma. The results demonstrate that enhanced image processing methods for segmentation give a robust system for optic disk segmentation.

2. Literature Review

Research on retinal image analysis has broadly focused on optic disc (OD) and optic cup (OC) segmentation, classical image processing approaches, deep learning frameworks, and multiple instance learning (MIL) methodologies. Almazroa et al. [1] provided a comprehensive survey of OD/OC segmentation methodologies, highlighting the clinical importance of the cup-to-disc ratio. Abdullah et al. [2] applied the circular Hough transform and the grow-cut algorithm for OD segmentation. In contrast, Rehman et al. [3] proposed a multi-parametric OD detection framework using superpixel-based feature classification. Ünver et al. [4] introduced statistical edge detection with CHT, and Ramani and Shanthamalar [5] refined optic disc segmentation with pixel density methods and red channel superpixels. Dietter et al. [6] developed a robust OD detection framework to handle strong artifacts. Zhao et al. [7] proposed SLIC superpixel-based disc segmentation. Fu et al. [8] demonstrated that deep learning achieves high agreement with manual OD/OC annotations, while Liu et al. [9] designed DDSC-Net to enhance OD/OC segmentation accuracy. Mahmood and Lee [10] localized OD using directional and radial blur analysis. Toptaş et al. [11] employed an optimized color space transformation, and Ali et al. [12] used vessel masking with the Hough transform for OD localization. Ávila et al. [13] proposed a superpixel-based ONH segmentation validated against experts, while Septiarini et al. [14] employed a CNN+U-Net pipeline for automatic OD segmentation. Jana and Sarkar [15] applied a mini-U-Net for vessel and OD segmentation.

The role of MIL in retinal disease detection is significant. Zhou et al. [16] and Papadopoulos et al. [17] applied MIL for DR detection using patch-level features and attention mechanisms. Bi et al. [18] proposed a local-global dual perception MIL, while Cao et al. [19] combined weakly supervised domain adaptation with MIL for DR grading. Mueller et al. [20] extended MIL to peripheral arterial disease detection, and Elmoufidi et al. [21] utilized deep learning with MIL for glaucoma prevention. Zhu et al. [22] reconciled MIL with self-supervised equivariant regularization for DR lesion segmentation. Bi et al. [23] proposed MIL-ViT, a vision transformer for fundus classification. Matten et al. [24] developed MIL-ResNet for OCTA images. Avolio et al. [25] presented MIL for DR detection. Li et al. [26] proposed lesion-patch MIL with semantic constraint adaptation. Fan et al. [27] designed a self-supervised refinement classification network for DR. Wei et al. [28] introduced MSTNet with MIL for DR classification. Lai et al. [29] integrated CNN and BLS into HybridMIL for medical image localization.

Methodological advances in MIL have been explored by Astorino et al. [30] through Lagrangian relaxation, while Avolio and Fuduli [31] proposed a semiproximal SVM for MIL. Avolio et al. [32] further applied MIL to DR detection, and Avolio and Fuduli [33] investigated kernel-based semiproximal SVM for MIL tasks. Collectively, these works demonstrate that traditional methods remain efficient for OD localization. Still, the shift towards deep learning and MIL approaches ensures scalability, robustness, and interpretability across glaucoma, DR, and other retinal and vascular diseases.

3. Methodology

Image segmentation serves as a core process in computer vision, aiming to divide an image into distinct regions based on specific areas of interest. Its primary objective is to group pixels or regions that exhibit similar characteristics, allowing for more precise analysis and understanding of the image content. This research primarily focuses on the optic disk segmentation from the retinal fundus image. Once the segmentation task is completed, image feature extraction is applied, followed by optimization algorithms to classify images. Overall pipeline of this research is illustrated in the following Figure 2

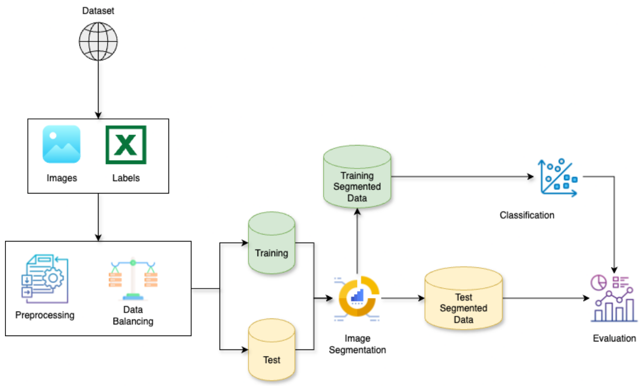

Figure 2. *Overall Pipeline..*

3.1. Data Acquisition

This study utilized the MESSIDOR dataset [34], a well-established resource for retinal image analysis. It contains 1,200 color fundus images collected from three French eye clinics. The images are labeled with expert-reviewed annotations indicating DR severity and macular edema risk. Among them, 898 images have a resolution of 1440×960 pixels, while 302 are 2240×1488, all in 8-bit RGB format. These properties make MESSIDOR suitable for segmentation and classification tasks in medical imaging.

3.2. Data Balancing

This study engaged a data balancing technique to ensure equal representation of classes. A simple random sampling method was applied, resulting in the selection of 200 images in total, with 100 from healthy patients and 100 from diseased patients.

3.3. Data Preprocessing

Data preprocessing is a crucial step in medical image analysis, particularly for segmentation tasks. In this study, preprocessing for the optic disc (OD) segmentation task involved single-channel extraction followed by image resizing to reduce computational complexity caused by high-dimensional images. All images were resized to 128×128 pixels.

3.4. Algorithm

This research is split into two parts: one is fundus image segmentation using image processing techniques, and the other is classification by Multiple Instance Learning approaches.

3.4.1. OD Segmentation

The optical disc (OD) is damaged when the glaucoma level of the human body is increased. So, the segmentation of the OD helps to view the more explicit anatomical changes in the optic nerve. To segment the optic disc (OD), the following procedure was applied: (1) clustering the RGB image using the superpixel method, (2) converting the image to grayscale, (3) applying Canny edge detection followed by morphological operations, (4) identifying circular structures using the Circular Hough Transform (CHT), and (5) refining the boundary with a convex hull.

3.4.2. SuperPixel

The optic disc (OD) region was estimated from fundus images using a superpixel-based approach. Superpixels are groups of pixels with similar characteristics, such as color, texture, or intensity, and they provide a more efficient representation of image structure compared to pixel-wise analysis. Given the non-uniform texture of fundus images, color-based clustering was employed for OD segmentation. The superpixel algorithm available in MATLAB was applied with two inputs: the RGB image and the number of superpixels, which was fixed at 300 in this study. Following superpixel generation, the mean value of each channel was computed to construct the clustered image.

Average values were calculated from the superpixel labels, where each label corresponded to a group of pixels. Since the optic disc (OD) region is represented by higher intensity values, close to white, the sorted pixel values played an essential role in its identification. After obtaining the clustered image, it was converted to grayscale, and the maximum intensity value was extracted by using (1).

$$I_{OC}(x,y) = \begin{cases} 1 & \text{if } I_{gray}(x,y) == I_{Max} \\ 0 & \text{Otherwise} \end{cases} \tag{1}$$

Where I_{OC} represents the output image optic cup (OC) after the superpixel approach, I_{gray} is the gray-scale image. From this value, the optic cup (OC) was identified, which was subsequently removed through a two-step procedure that includes the global Otsu's method and considers the largest blob.

3.4.3. Circular Haugh Transformation

The Circular Hough Transform (CHT) is widely used to identify circular objects within an image. Its main advantage lies in its ability to detect circular shapes of varying sizes and positions. The mathematical formulation of CHT is expressed as (2)

$$c = \sqrt{(x-a)^2 + (y-b)^2} \tag{2}$$

where a and b represent the center of the circle and c represents the radius. In this study, CHT was applied to the optic cup (OC) image following several steps. First, Canny edge detection was performed to highlight boundary pixels. Next, the radius was fixed, and non-zero pixels were extracted to calculate the minimum and maximum distances along the x-axis. Based on these x-positions, the corresponding y-positions were determined, allowing circles to be drawn accordingly. Finally, the pixel with maximum intensity was considered the center, from which the optic disc boundary was outlined.

3.4.4. Multiple Instance Learning

Multiple Instance Learning (MIL) is a machine learning paradigm in which data is organized into groups, referred to as bags, each comprising multiple elements known as instances. Unlike traditional supervised learning, labels are assigned only at the bag level rather than for individual instances. This research explicitly used MIL and different MIL algorithms to classify images. The algorithms that is used to classify images in this research are MIL-RL [30], mi-SPSVM [31], mi-KSPSVM [33], SVM, and SVM (RBF). Mathematically, mi-SPSVM is defined as (3):

$$\begin{cases} \min\limits_{w,b,\epsilon} \frac{1}{2}(w^T w + b^2) + \frac{C}{2}\sum\limits_{i=1}^{m}\sum\limits_{j\in J_i^+} ||\epsilon_j||^2 + C\sum\limits_{i=1}^{k}\sum\limits_{j\in J_i^-}\psi_j \\ \epsilon_j = 1-(w^T x_j + b) \quad j\in J_i^+, i=1,...,m \\ \psi_j \geq 1 + (w^T x_j + b) \quad j \in J_l^-, l=1,...,k \\ \psi_j \geq 0 \quad j\in J_l^-, l=1,...,k \end{cases} \tag{3}$$

On the other hand, MIL-RL is defined as (4):

$$\begin{cases} \min\limits_{w,b,y,\epsilon,\psi} \quad \frac{1}{2}||w||^2 + C\sum\limits_{i=1}^{m}\sum\limits_{j\in J_i^+}\epsilon_j + C\sum\limits_{i=1}^{k}\sum\limits_{j\in J_i^-}\psi_j \\ \qquad \epsilon_j \geq 1 - y_j(w^T x_j + b) \quad j\in J_i^+, i=1,...,m \\ \qquad \psi_j \geq 1+(w^T x_j + b) \quad j\in J_l^-, l=1,...,k \\ \qquad \sum\limits_{j\in J_i^+}\frac{y_j+1}{2} \geq 1, i=1...m \\ \qquad y_j \in \{-1,+1\}, \quad j\in J_i^+, i=1...m \\ \qquad \epsilon_j \geq 0 \quad j \in J_i^+, i=1,...,m \\ \qquad \psi_j \geq 0 \quad j\in J_l^-, l=1,...,k \end{cases} \tag{4}$$

Subsequently, mi-KSPSVM is defined as (5):

$$\begin{cases} \min\limits_{\lambda,\mu} \quad \frac{1}{2}\Bigg(\sum\limits_{i=1}^{m}\sum\limits_{j\in J_i^+}\lambda_i\lambda_j\phi(x_i)^T\phi(x_j) \\ \qquad - 2\sum\limits_{i=1}^{m}\sum\limits_{l=1}^{k}\lambda_i\mu_l\phi(x_i)^T\phi(x_l) \\ \qquad + \sum\limits_{l=1}^{k}\sum\limits_{j\in J_l^-}\mu_l\mu_j\phi(x_l)^T\phi(x_j)\Bigg) \\ \qquad + \frac{1}{2}\Bigg(\sum\limits_{i=1}^{m}\sum\limits_{j\in J_i^+}\lambda_j - \sum\limits_{l=1}^{k}\sum\limits_{j\in J_i^-}\mu_j\Bigg)^2 \\ \qquad - \frac{\left(\sum_{i=1}^{m}\sum_{j\in J_i^+}\lambda_j\right)^2}{2C} + \sum\limits_{i=1}^{m}\sum\limits_{j\in J_i^+}\lambda_j + \sum\limits_{l=1}^{k}\sum\limits_{j\in J_i^-}\mu_j \\ \qquad 0\leq \mu_j \leq C, \quad j\in J_i^-, i=1,...,k \end{cases} \tag{5}$$

3.5. Evaluation

This section outlines the evaluation process for models. To evaluate the model's performance in an unseen scenario, the following matrices were calculated:

1. *Testing Correctness (TC):* The assessment of the model's accuracy in accurately identifying medical images is called "testing correctness in medical image classification." It involves comparing the test dataset's ground-truth labels with the predicted labels generated by the classification model. The equation of testing correctness is:

$$\text{TC} = \frac{\text{\# of correctly classified in the testing set}}{\text{\# total points in the testing set}}$$

2. *Sensitivity:* Sensitivity represents the ratio of positive images correctly classified to the actual positive images. It evaluates how well the model detects positive examples and is often referred to as sensitivity. To calculate the sensitivity of a model, the following:

$$\text{Sensitivity} = \frac{\text{\# of positive images correctly classified}}{\text{\# actual positive images}}$$

3. *Specificity:* Specificity calculates the proportion of correctly predicted negative (true negative) images among all the actual negative images. It assesses the model's ability to identify negative cases accurately. To calculate the specificity of a model, the following:

$$\text{Specificity} = \frac{\text{\# of negative images correctly classified}}{\text{\# actual negative images}}$$

4. *Precision:* Precision measures the fraction of accurate optimistic predictions out of all instances that the model has labeled as positive. Reflects the model's accuracy in identifying positive cases.

$$\text{Precision} = \frac{\text{\# of positive images correctly classified}}{\text{\# total points classified as positive}}$$

5. *F1-Score:* F1 Score is the inverse of the arithmetic mean of precision and sensitivity. Provides a balanced measure that considers both precision and recall.

$$\text{F1-Score} = 2 \times \frac{\text{sensitivity} \times \text{precision}}{\text{sensitivity} + \text{precision}}$$

4. Results

The experimental evaluation in this study was conducted using two approaches: one without preprocessing of the images and the other with preprocessing applied. To examine potential differences between the two approaches, the models were tested on the prepared dataset using 5-fold, 10-fold, and leave-one-out cross-validation (LOOCV). After obtaining the results, sensitivity was given primary consideration, as it reflects the ability to classify positive cases correctly. In addition, testing accuracy, specificity, F1-score, and CPU time were also evaluated. The detailed numerical results are presented below.

4.1. Without Preprocessed Image

The first experiment on diabetic retinopathy disease was conducted without image processing, where a full image is considered and applied to all five models, and then used for inference. Table 1 illustrates experiment results.

Table 1. *Performance metrics of a full fundus image (without segmentation).*

Cross Validation	Model	Correctness(%)	Sensitivity(%)	Specificity(%)	F1-Score(%)	CPU Time(s)
	mi-KSPSVM	55.50	78.32	33.13	63.52	0.27
	mi-SPSVM	53.50	74.47	33.41	61.40	0.67
5-Fold	MIL-RL	49.50	8.21	91.06	11.64	9.33
	SVM	47.50	35.54	57.76	38.88	1.51
	SVM (RBF)	58.50	62.64	54.17	59.93	0.28
	mi-KSPSVM	55.50	76.18	33.24	62.69	0.18
	mi-SPSVM	54.00	76.07	32.60	61.61	0.33
10-Fold	MIL-RL	48.00	12.66	86.67	10.38	14.94
	SVM	50.00	43.58	56.63	45.06	1.57
	SVM (RBF)	57.00	62.15	54.04	58.49	0.09
	mi-KSPSVM	52.00	79.00	25.00	62.20	0.36
	mi-SPSVM	54.50	74.00	35.00	61.92	2.84
LOO	MIL-RL	39.50	52.00	27.00	46.22	20.94
	SVM	47.50	38.00	57.00	41.99	1.64
	SVM (RBF)	55.50	58.00	53.00	56.59	0.02

4.2. With Preprocessed Image

After evaluating the model using images without segmentation, the second step was to repeat the process with segmented images. This step is the same as the previous steps. Table 2 illustrates experiment results.

Table 2. *Performance metrics of a full fundus segmented image.*

Cross Validation	Model	Testing Correctness(%)	Sensitivity(%)	Specificity(%)	F1-Score(%)	CPU Time(s)
	mi-KSPSVM	52.50	77.56	29.12	61.96	0.09
	mi-SPSVM	55.50	87.06	24.33	66.17	0.54
5-Fold	MIL-RL	56.00	47.32	65.71	50.24	11.09
	SVM	61.50	50.83	72.94	56.42	1.31
	SVM (RBF)	48.50	56.94	40.86	50.95	0.17
	mi-KSPSVM	49.50	78.83	23.63	60.15	0.11
	mi-SPSVM	56.50	90.00	24.15	67.09	0.23
10-Fold	MIL-RL	52.00	32.61	73.65	37.62	10.83
	SVM	57.50	55.83	63.30	55.32	1.36
	SVM (RBF)	47.50	52.35	43.24	48.43	0.10
	mi-KSPSVM	48.50	81.00	16.00	61.13	0.15
	mi-SPSVM	54.50	83.00	26.00	64.59	1.28
LOO	MIL-RL	47.50	36.00	59.00	40.68	17.05
	SVM	61.50	47.00	76.00	54.97	1.39
	SVM (RBF)	49.00	56.00	42.00	52.34	0.02

4.3. Quantitative Analysis

The above two tables present the performance metrics of multiple classification models evaluated on full fundus images without segmentation and with optic disc (OD) segmentation, respectively, under 5-fold, 10-fold, and leave-one-out (LOO) cross-validation schemes.

In the case of images without segmentation, performance altered across models and validation strategies. For 5-fold cross-validation, SVM with an RBF kernel achieved the highest testing correctness (58.50%) with congruous sensitivity (62.64%) and specificity (54.17%). MIL-RL, however, showed significantly poor sensitivity (8.21%) but strong specificity (91.06%), indicating a strong bias toward negative cases. Under 10-fold validation, SVM (RBF) again achieved competitive correctness (57.00%), while MIL-RL stayed weak in sensitivity (12.66%). For LOO validation, correctness values generally decreased, with mi-SPSVM performing best at 54.50% but still limited in specificity (35.00%). Overall, models trained on unsegmented images demonstrated unstable and imbalanced performance across sensitivity and specificity.

In contrast, images with segmentation preprocessing produced more stable and improved outcomes. For 5-fold validation, SVM achieved the highest testing correctness (61.50%) and specificity (72.94%), while mi-SPSVM recorded the best sensitivity (87.06%) and F1-score (66.17%). CPU time was minimal for mi-KSPSVM (0.09s), highlighting its computational efficiency. Under 10-fold validation, SVM again delivered the best correctness (57.50%) and strong specificity (63.30%), while mi-SPSVM provided the best sensitivity (90.00%) and F1-score (67.09%). For LOO, mi-SPSVM preserved the highest sensitivity (83.00%) and F1-score (64.59%), whereas SVM achieved the best correctness (61.50%) and specificity (76.00%). Computational efficiency remained highest for mi-KSPSVM and SVM(RBF), with runtimes below 0.15s.

When comparing the two approaches, segmentation unfailingly improved classification metrics. On average, testing correctness increased by approximately 3-4% for SVM (from 47.50-50.00% without segmentation to 57.50-61.50% with segmentation). Similarly, sensitivity improved by 8-12% for SVM-based methods after segmentation, while mi-SPSVM achieved a maximum sensitivity of 15.53% (from 74.47% to 90.00%). Specificity was also enhanced, with SVM reaching 76.00% with segmentation compared to 57.76% without segmentation in LOO validation. F1-scores increased across nearly all models, with mi-SPSVM showing the highest growth of almost 6% (from 61.40% to 67.09%).

Altogether, the results reveal that OD segmentation preprocessing not only improves classification accuracy but also declines the trade-off between sensitivity and specificity. Models such as SVM and mi-SPSVM yielded the best results, achieving strengths across correctness, sensitivity, and F1-score, whereas MIL-RL remained biased despite some specificity growth.

4.4. Comparative Analysis

In addition, a qualitative analysis of sensitivity related to different optimization models was performed. The bar graphs in Figures 3,4,5 present a comparative analysis showing that preprocessing consistently improves sensitivity across all models. In the 5-fold CV results, mi-SPSVM outperforms all models, while mi-KSPVM performs significantly lower than mi-SPSVM.

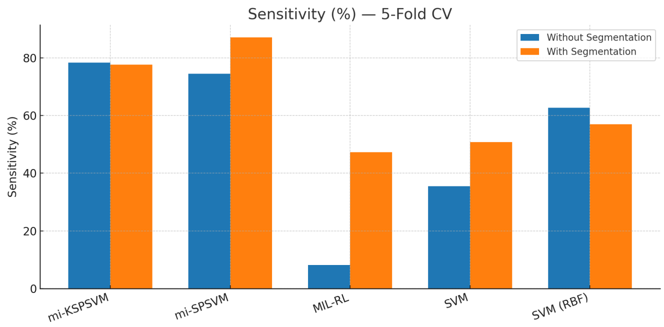

Figure 3. Qualitative Analysis of Sensitivity over 5-Fold Cross-Validation.

From the 10-fold CV results, mi-SPSVM, MIL-RL, and SVM show consistency over sensitivity. However, mi-KSPSVM performs significantly higher than previous performance.

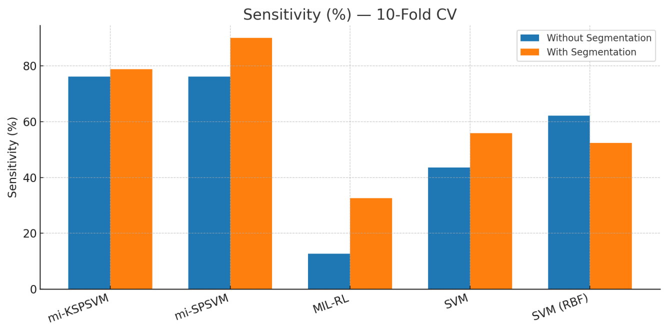

Figure 4. Qualitative Analysis of Sensitivity over 10-Fold Cross-Validation.

In LOOCV, it clearly indicates that multiple instance-based SPSVM and KSPSVM outperform all other models. Where SVM is consistent in three validation stages.

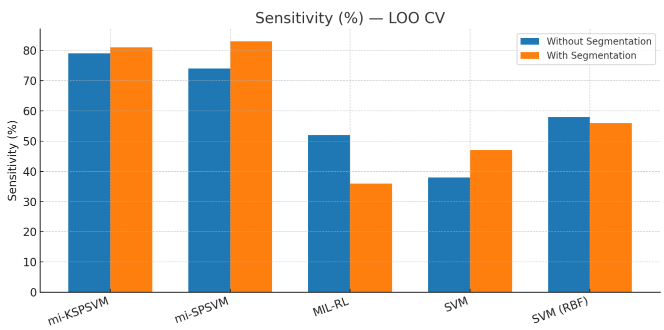

Figure 5. Qualitative Analysis of Sensitivity over LOO Cross-Validation.

4.5. Discussion

This study underscores the optic disk (OD) segmentation as a crucial preprocessing step for retinal fundus image classification. The segmentation was performed using standard image processing techniques, ensuring that the OD region was accurately localized while keeping essential anatomical details. This strategy not only improves the reliability of the following classification but also reveals that lightweight segmentation pipelines can be both computationally efficient and practically achievable.

All experiments were performed on a Mac OS system provided with an M1 processor and 8GB RAM, emphasizing the feasibility of achieving stable and meaningful outcomes without support for GPU acceleration. This highlights the suitability of the proposed approach for research and deployment in environments with limited computational resources.

Although traditional image processing techniques may not capture the full range of pathological deviations as effectively as advanced deep learning models, they remain useful due to faster performance, lower memory requests, and ease of implementation. The findings confirm that a segmentation-driven framework can serve as a reliable foundation for the classification of retinal fundus images, particularly in resource-constrained environments where efficiency and practicality are essential.

5. Conclusion

In this research, a robust and efficient optic disk segmentation approach is developed that utilizes image processing techniques, including image preprocessing, superpixels, and circular haugh transformation, that is especially designed for retinal diseases. Apart from image segmentation, this research also entails an approach to classify images using linear and nonlinear multiple instance learning. After rigorous testing, it indicates that instead of using a full fundus image, a segmented image is significantly better in all aspects, particularly in terms of sensitivity and computational time, where low resource is required. However, more research is necessary to improve the overall performance. This entails an alternative technique in the segmentation task to enhance classification accuracy, as well as a method to improve the applicability of retinal disease detection to other aspects. Recently developed deep learning based approaches could be included in this research to facilitate the segmentation process in a more efficient way, which will have an impact on classification using MIL approaches. Also, in MIL, another potential direction of the research is to test the effectiveness of the proposed method in other medical fields to detect more types of skin cancer lesions.

ORCID

0009-0000-7906-1823 (Mahbub Hasan)

Abbreviations

DRD	Diabetic Retinopathy Disease
DME	Diabetic Macular Edema
OD	Optic Disk
TC	Testing Correctness
CV	Cross Validation
LOO	Leave-One-Out
MIL	Multiple Instance Learning
SVM	Support Vector Machine
MIL-RL	Multiple Instance Learning With Lagrangian Relaxation
mi-SPSVM	Multiple Instance, Semiproximal Support Vector Machine
mi-KSPSVM	Multiple Instance, Kernel-based Semiproximal Support Vector Machine
CHT	Circular Haugh Transformation

Conflicts of Interest

The author declares no conflicts of interest.

References

[1] Almazroa, A., Burman, R., Raahemifar, K., & Lakshminarayanan, V. (2015). Optic Disc and Optic Cup Segmentation Methodologies for Glaucoma Image Detection: A Survey. Journal of ophthalmology, 2015, 180972. https://doi.org/10.1155/2015/180972

[2] Abdullah, M., Fraz, M. M., & Barman, S. A. (2016). Localization and segmentation of optic disc in retinal images using circular Hough transform and grow-cut algorithm. PeerJ, 4, e2003. https://doi.org/10.7717/peerj.2003

[3] Rehman, Z. U., Naqvi, S. S., Khan, T. M., Arsalan, M., Khan, M. A., & Khalil, M. A. (2019). Multi-parametric optic disc segmentation using superpixel based feature classification. Expert Systems with Applications, 120, 461-473. https://doi.org/10.1016/j.eswa.2018.12.008

[4] Ünver, H. M., Kökver, Y., Duman, E., & Erdem, O. A. (2019). Statistical Edge Detection and Circular Hough Transform for Optic Disk Localization. Applied Sciences, 9(2), 350. https://doi.org/10.3390/app9020350

[5] Ramani, R. G., & Shanthamalar, J. J. (2020). Improved image processing techniques for optic disc segmentation in retinal fundus images. Biomedical Signal Processing and Control, 58, 101832. https://doi.org/10.1016/j.bspc.2019.101832

[6] Dietter, J., Haq, W., Ivanov, I. V., Norrenberg, L. A., Völker, M., Dynowski, M., ... & Ueffing, M. (2019). Optic disc detection in the presence of strong technical artifacts. Biomedical Signal Processing and Control, 53, 101535. https://doi.org/10.1016/j.bspc.2019.04.012

[7] Zhao, X., Wang, H., & Peng, Z. (2019, December). Fine segmentation of fundus optic disc based on SLIC superpixel. In AOPC 2019: AI in Optics and Photonics (Vol. 11342, pp. 155-163). SPIE. https://doi.org/10.1117/12.2547992

[8] Fu, H., Li, F., Xu, Y., Liao, J., Xiong, J., Shen, J., ... & iChallenge-GON study group. (2020). A retrospective comparison of deep learning to manual annotations for optic disc and optic cup segmentation in fundus photographs. Translational vision science & technology, 9(2), 33-33. https://doi.org/10.1167/tvst.9.2.33

[9] Liu, B., Pan, D. & Song, H. Joint optic disc and cup segmentation based on densely connected depthwise separable convolution deep network. BMC Med Imaging 21, 14 (2021). https://doi.org/10.1186/s12880-020-00528-6

[10] Mahmood, M. T., & Lee, I. H. (2022). Optic disc localization in fundus images through accumulated directional and radial blur analysis. Computerized Medical Imaging and Graphics, 98, 102058. https://doi.org/10.1016/j.compmedimag.2022.102058

[11] Toptaş, B., Toptaş, M. & Hanbay, D. Detection of Optic Disc Localization from Retinal Fundus Image Using Optimized Color Space. J Digit Imaging 35, 302-319 (2022). https://doi.org/10.1007/s10278-021-00566-8

[12] Ali A, Wan Zaki WMD, Hussain A et al. Vessel masking and Hough transform for optic disc localisation from retinal images [version 1; peer review: 1 approved with reservations, 1 not approved]. F1000Research 2022, 11: 181 https://doi.org/10.12688/f1000research.73390.1

[13] Ávila, F. J., Bueno, J. M., & Remón, L. (2022). Superpixel-Based Optic Nerve Head Segmentation Method of Fundus Images for Glaucoma Assessment. Diagnostics, 12(12), 3210. https://doi.org/10.3390/diagnostics12123210

[14] Septiarini, A., Hamdani, H., Setyaningsih, E., Junirianto, E., & Utaminingrum, F. (2023). Automatic method for optic disc segmentation using deep learning on retinal fundus images. Healthcare Informatics Research, 29(2), 145-151. https://doi.org/10.4258/hir.2023.29.2.145

[15] Jana, S., & Sarkar, P. (2024). Optic Disc and Vessel Segmentation from Fundus Image using Miniunet Architecture. medRxiv, 2024-12. https://doi.org/10.1101/2024.12.28.24319728

[16] Zhou, L., Zhao, Y., Yang, J., Yu, Q., & Xu, X. (2018). Deep multiple instance learning for automatic detection of diabetic retinopathy in retinal images. IET Image Processing, 12(4), 563-571. https://doi.org/10.1049/iet-ipr.2017.0636

[17] Papadopoulos, A., Topouzis, F., & Delopoulos, A. (2021). An interpretable multiple-instance approach for the detection of referable diabetic retinopathy in fundus images. Scientific Reports, 11(1), 14326. https://doi.org/10.1038/s41598-021-93632-8

[18] Bi, Q. et al. (2021). Local-Global Dual Perception Based Deep Multiple Instance Learning for Retinal Disease Classification. In: de Bruijne, M., et al. Medical Image Computing and Computer Assisted Intervention - MICCAI 2021. MICCAI 2021. Lecture Notes in Computer Science (), vol 12908. Springer, Cham. https://doi.org/10.1007/978-3-030-87237-3_6

[19] Cao, P., Hou, Q., Song, R., Wang, H., & Zaiane, O. (2022). Collaborative learning of weakly-supervised domain adaptation for diabetic retinopathy grading on retinal images. Computers in Biology and Medicine, 144, 105341. https://doi.org/10.1016/j.compbiomed.2022.105341

[20] Mueller, S., Wintergerst, M. W., Falahat, P., Holz, F. G., Schaefer, C., Schahab, N., ... & Schultz, T. (2022). Multiple instance learning detects peripheral arterial disease from high-resolution color fundus photography. Scientific Reports, 12(1), 1389. https://doi.org/10.1038/s41598-022-05169-z

[21] Elmoufidi, A., Skouta, A., Jai-Andaloussi, S., & Ouchetto, O. (2022). Deep multiple instance learning for automatic glaucoma prevention and auto-annotation using color fundus photography. Progress in Artificial Intelligence, 11(4), 397-409. https://doi.org/10.1007/s13748-022-00292-4

[22] Zhu, W., Qiu, P., Lepore, N., Dumitrascu, O. M., & Wang, Y. (2023, March). Self-supervised equivariant regularization reconciles multiple-instance learning: Joint referable diabetic retinopathy classification and lesion segmentation. In 18th International Symposium on Medical Information Processing and Analysis (Vol. 12567, pp. 100-107). SPIE. https://doi.org/10.1117/12.2669772

[23] Bi, Q., Sun, X., Yu, S., Ma, K., Bian, C., Ning, M., ... & Zheng, Y. (2023). MIL-ViT: A multiple instance vision transformer for fundus image classification. Journal of Visual Communication and Image Representation, 97, 103956. https://doi.org/10.1016/j.jvcir.2023.103956

[24] Matten, P., Scherer, J., Schlegl, T., Nienhaus, J., Stino, H., Niederleithner, M., ... & Schmoll, T. (2023). Multiple instance learning based classification of diabetic retinopathy in weakly-labeled widefield OCTA en face images. Scientific Reports, 13(1), 8713. https://doi.org/10.1038/s41598-023-35713-4

[25] Avolio, M., Fuduli, A., Vocaturo, E., & Zumpano, E. (2023). Multiple Instance Learning for Diabetic Retinopathy Detection. In SEBD (pp. 22-31). https://www.semanticscholar.org/paper/Multiple-Instance-Learning-for-Diabetic-Retinopathy-Avolio-Fuduli/239d08976fe53b4b795a3f81b5fc2163074d722b

[26] Li, R., Gu, Y., Wang, X., & Pan, J. (2023). A Cross-Domain Weakly Supervised Diabetic Retinopathy Lesion Identification Method Based on Multiple Instance Learning and Domain Adaptation. Bioengineering, 10(9), 1100. https://doi.org/10.3390/bioengineering10091100

[27] Fan, J., Yang, T., Wang, H., Zhang, H., Zhang, W., Ji, M., & Miao, J. (2025). A self-supervised equivariant refinement classification network for diabetic retinopathy classification. Journal of Imaging Informatics in Medicine, 38(3), 1796-1811. https://doi.org/10.1007/s10278-024-01270-z

[28] Wei, X., Liu, Y., Zhang, F., Geng, L., Shan, C., Cao, X., & Xiao, Z. (2025). MSTNet: Multi-scale spatial-aware transformer with multi-instance learning for diabetic retinopathy classification. Medical Image Analysis, 102, 103511. https://doi.org/10.1016/j.media.2025.103511

[29] Lai, Q., Vong, C. M., Yan, T., Wong, P. K., & Liang, X. (2025). Hybrid multiple instance learning network for weakly supervised medical image classification and localization. Expert Systems with Applications, 260, 125362. https://doi.org/10.1016/j.eswa.2024.125362

[30] Astorino, A., Fuduli, A. and Gaudioso, M., 2019. A Lagrangian relaxation approach for binary multiple instance classification. IEEE transactions on neural networks and learning systems, 30(9), pp.2662-2671. https://doi.org/10.1109/TNNLS.2018.2885852

[31] Avolio, M. and Fuduli, A., 2020. A semiproximal support vector machine approach for binary multiple instance learning. IEEE transactions on neural networks and learning systems, 32(8), pp.3566-3577. https://doi.org/10.1109/TNNLS.2020.3015442

[32] Avolio, M., Fuduli, A., Vocaturo, E. and Zumpano, E., 2023, May. On detection of diabetic retinopathy via multiple instance learning. In Proceedings of the 27th International Database Engineered Applications Symposium (pp. 170-176). https://doi.org/10.1145/3589462.3589490

[33] Avolio, M. and Fuduli, A., 2024. The semiproximal SVM approach for multiple instance learning: a kernel-based computational study. Optimization Letters, 18(2), pp.635-649. https://doi.org/10.1007/s11590-023-02022-8

[34] Decencière, Etienne and Zhang, Xiwei and Cazuguel, Guy and Lay, Bruno and Cochener, Béatrice and Trone, Caroline and Gain, Philippe and Ordóñez-Varela, John-Richard and Massin, Pascale and Erginay, Ali, 2014. Feedback on a publicly distributed image database: the Messidor database. Image Analysis & Stereology, pp.231-234. https://doi.org/10.5566/ias.1155